Non biogenic source is an important but overlooked contributor to aerosol isoprene-derived organosulfates during winter in northern China

Ting Yang[1], Yu Xu[1,2]*, Yu-Chen Wang[3], Yi-Jia Ma[1], Hong-Wei Xiao[1,2], Hao Xiao[1,2], Hua-Yun Xiao[1,2]

[1]School of Agriculture and Biology, Shanghai Jiao Tong University, Shanghai 200240, China

[2]Shanghai Yangtze River Delta Eco-Environmental Change and Management Observation and Research Station, Ministry of Science and Technology, Ministry of Education, Shanghai 200240, China

[3]Division of Environment and Sustainability, Hong Kong University of Science and Technology, Hong Kong SAR 00000, China

*Corresponding authors

Yu Xu

E-mail: xuyu360@sjtu.edu.cn

Abstract: Previous measurement-model comparisons of atmospheric isoprene levels showed a significant unidentified source of isoprene in some northern Chinese cities during winter. Here, spatial variability in winter aerosol organosulfate (OS) formation in typical southern (Guangzhou and Kunming) and northern (Xi'an and Taiyuan) cities, China, was investigated to reveal the influence of potential non biogenic contributor on aerosol OS pollution levels. Monoterpene-derived OSs were significantly higher in southern cities than in northern cities, which was attributed to temperature dependent emission of monoterpenes (i.e., higher temperatures in southern cities drove more monoterpene emissions). However, isoprene-derived OSs (OS_i) showed the opposite trend, with significantly higher levels in northern cities. Principal component analysis combined with field simulation combustion experiments suggested that biomass burning rather than gasoline, diesel, and coal combustion contributed significantly to the abundance of OS_i in northern cities. The comparison of anthropogenic OS molecular characteristics between particles released from various combustion sources and ambient aerosol particles suggested that stronger biomass and fossil fuel combustion activities in northern cities promoted the formation of considerable anthropogenic OSs. Overall, this study provides direct molecular evidence for the first time that non biogenic sources can significantly contribute to the formation of OS_i in China during winter.

Keywords: Aerosol organosulfates, Biogenic precursors, Anthropogenic precursors, Spatial variation, Influencing factors, Biomass burning

1. Introduction

Organosulfates (OSs) with a sulfate ester functional group typically contribute 3–30% of the organic aerosol mass in atmospheric fine particles ($PM_{2.5}$) (Luk´Acs et al. 2009). Moreover, OSs have been estimated to account for up to 12% of the total sulfur mass in fine particles, playing significant roles in the global biogeochemical cycling of sulfur (Luk´Acs et al. 2009). In particular, OSs can impact the properties of aerosols, such as hygroscopicity, acidity, viscosity, and morphology, which are closely associated with the organic aerosol formation and urban air quality (Riva et al. 2019; Fleming et al. 2019). Thus, aerosol OSs have attracted significant attention over the years. However, the mechanisms and key factors impacting the formation and abundance of aerosol OSs in the real world remain considerable uncertainty, despite the important insights gained from laboratory simulation experiments (Wang et al. 2021; Yang et al. 2023; Wang et al. 2020).

Previous field studies have indicated that acidity (Duporté et al. 2019), sulfate (Aoki et al. 2020), aerosol liquid water (Duporté et al. 2016), and oxidants (e.g., ozone) (Wang et al. 2021) represent critical factors controlling the formation of OSs via heterogeneous and liquid phase processes (Brüggemann et al. 2020b). Precursor emission intensities (e.g., isoprene, monoterpenes, polycyclic aromatic hydrocarbons, and alkanes) also play an important role in impacting abundance of biogenic and anthropogenic OSs in ambient aerosols (Wang et al. 2022; Bryant et al. 2021; Yang et al. 2024). Furthermore, previous studies have identified a large number of CHOS compounds in smoke particles (e.g., pine branches, corn straw, rice straw, and coal)

(Song et al. 2019; Song et al. 2018; Tang et al. 2020). However, limited studies have focused on the contribution of different smoke particles to urban aerosol OSs. This may be an overlooked source of OSs. In general, few field studies have conducted a comprehensive investigation into the relationship between biogenic and anthropogenic impacting factors and regional differences in aerosol OS pollution. This complicates our understanding of how aerosol OS pollution is formed and what limits it in a complex polluted atmosphere across different cities in China.

The considerable variations in climatic conditions and air pollution levels in the northern and southern regions of China during winter (Ding et al. 2014; Ding et al. 2016b) provide a distinctive opportunity to examine the complex influences of precursors, humidity, acidity, atmospheric oxidants, and anthropogenic pollution on the formation and abundance of aerosol OSs in the real world (Yang et al. 2024; Yang et al. 2023; Wang et al. 2021; Hettiyadura et al. 2019). In this study, we conducted the simultaneous observations of OSs and other chemical components in $PM_{2.5}$ collected from typical southern (Guangzhou and Kunming) and northern (Xi'an and Taiyuan) cities in China during winter. Moreover, we also attempted to identify OSs in smoke particles emitted from combustion of different materials (i.e., rice straw, pine branch, diesel, gasoline, and coal). The principal aims of this study are 1) to investigate the spatial differences in aerosol OS pollution in northern and southern China during winter and 2) to elucidate the key factors that contribute to the spatial variability of OS pollution, with a focus on the OSs derived from smoke particles.

2. Materials and Methods

2.1. Site description and sample collection

The research sites are located in four urban areas in China, including Xi'an (XA) Taiyuan (TY), Guangzhou (GZ), and Kunming (KM) (**Figure S1a**). XA and TY are typical northern cities with cold winters (average temperature below 2 ℃ during the study period; **Table S1**). Thus, burning coal and biomass for heating is prevalent in these two cities during winter (Zhou et al. 2017; Ma et al. 2017), which significantly deteriorated the local air quality (**Figure S1b**). GZ and KM represent typical southern cities, with an average air temperature of over 10 ℃ during the winter sampling period (**Table S1**). Clearly, the distinctive climatic conditions in the northern and southern cities during winter may lead to significant spatial differences in the level of air pollution and the emission intensity of biogenic volatile organic compounds (VOCs) (Ding et al. 2014; Xu et al. 2024b).

From 10 December 2017 to 8 January 2018, sampling was performed simultaneously in four cities. Filters contained $PM_{2.5}$ were collected at regular two- to three-day intervals, with the collection duration being 24 hours, using a high-volume air sampler (Series 2031, Laoying, China) at a flow rate of ~1.05 m^3 min^{-1} (Xu et al. 2024a). A blank filter was sampled at each of the study sites. A total of 48 ambient samples were collected and stored at a temperature of −30°C. Meteorological data, including wind speed, relative humidity (RH), and temperature, were obtained from nearby environmental stations. Concurrently, the concentrations of various pollutants, such as O_3, NO_2, and SO_2, were also recorded.

2.2. Smoke particle collection

The controlled burning experiments conducted in the field were designed to simulate the emissions of "real world" burning cases in China (**Figure S2**), with the methodology being improved according to the previous reports (He et al. 2010; Wang et al. 2017). Rice straw and pine branch are typical materials for biomass burning in China (Zhou et al. 2017). In addition, the combustion of coal, gasoline, and diesel was representative of fossil fuel combustion (Yu et al. 2020). Accordingly, the smoke particles emitted from rice straw, pine branch, coal combustion, gasoline vehicle exhausts, and diesel vehicle exhausts were separately collected using self-made devices (**Figure S2**).

Briefly, the smoke from the combustion of rice straw, pine branch, and coal was sampled through a combustion furnace pumped with ambient air (particulate matter is removed) (**Figure S2a**). It should be noted that introducing ambient air with removed particulate matter into the combustion furnace is to minimize the pollution of ambient particulate matter to the smoke particle samples. Each combustion experiment for straw, pine branch, and coal lasted for 30−40 min. Regarding the smoke particles emitted from gasoline vehicle exhausts and diesel vehicle exhausts, they were collected for 3 hours by directly connecting to the car exhaust pipe (**Figure S2b**). All smoke particle samples are collected onto prebaked quartz fiber filters via a high-volume air sampler (Series 2031, Laoying, China). Four repeated experiments were conducted for each combustion material, one of which was collected as a blank sample. All smoke particle samples were stored at −30°C.

2.3. Chemical analysis and predictions of aerosol acidity and water concentration

The extraction, measurement procedures, and identification of OSs were described in detail in our recent publications (Yang et al. 2024). Briefly, the filter sample was extracted using methanol, then filtered through a 0.22 μm PTFE syringe filter and concentrated by a gentle stream of nitrogen gas. Subsequently, the concentrated sample with adding ultrapure water (300 μL) was thoroughly mixed using a mixer. The mixture was centrifuged to obtain the supernatant for analysis of UPLC-MS/MS system (Waters, USA) (Wang et al. 2021). The reverse-phase liquid chromatography (RPLC) method was performed on an Acquity UPLC HSS T3 column (2.1mm × 100 mm, 1.8 μm particle size; Waters, USA) in this study. Although our method is quite effective in retaining and separating low molecular weight (MW) OSs, as demonstrated in our recent publication (Yang et al. 2024), we also acknowledge that the developed hydrophilic interaction liquid chromatography method may provide another solution for the measurement of low-MW OSs (Cui et al. 2018; Hettiyadura et al. 2015).

In addition, it has been indicated in previous studies (Brüggemann et al. 2020a; Kristensen et al. 2016) that the levels of OSs can be affected by the sampling procedure, especially when SO_2 removal procedures are not employed. On the assumption that SO_2 reacts with organics on filters to form OSs, similar processes must also occur on ambient particles prior to sampling. Moreover, there is currently no study evaluating the relative efficiency of OS generation in filters and ambient particles. Consequently, the possible consequences of sampling without denuding SO_2

for the quantification of OSs were not taken into account in our studies (Yang et al. 2024; Yang et al. 2023). In total, 212 OSs were identified. However, only 111 OS species were quantified using surrogate standards in this study (**Table S2** and **S3**). The study divided the several principal OS groups as follows: monoterpene-derived OSs (OS_m), isoprene-derived OSs (OS_i), C_2−C_3 OSs (i.e., OSs with two or three carbon atoms), and anthropogenic OSs (i.e, aliphatic and aromatic OSs) (Yang et al. 2023). The terms "OS_m" and "OS_i" refer to organosulfates generated from monoterpenes and isoprene, respectively. These compounds were generally classified as biogenic OSs due to their natural origin (Wang et al. 2021; Wang et al. 2018). The specific classification and quantification methods were detailed in our recent publications (Yang et al. 2023; Yang et al. 2024) and **Supporting Information**.

An additional portion of each filter was extracted using ultrapure water for determining the inorganic ions (Huang et al. 2023). The concentrations of SO_4^{2-}, Ca^{2+}, NO_3^-, Na^+, K^+, Mg^{2+}, Cl^-, and NH_4^+ were analyzed using ICS5000+ ion chromatography (Thermo, USA) (Yang et al. 2024; Lin et al. 2023). The mass concentration of aerosol liquid water (ALW) and pH value were calculated by a thermodynamic model (ISORROPIA-II) in the forward mode and thermodynamically metastable state, which was detailed in our previous studies (Liu et al. 2023; Xu et al. 2022; Xu et al. 2023b; Xu et al. 2020). The influence of OSs on ALW and pH was not taken into account in the present study due to their negligible contribution to the prediction outcomes, as indicated by Riva et al. (2019) and Yang et al. (2024).

3. Results and Discussion

3.1. Spatial variations in concentrations and compositions of different OSs

Figure 1a shows the spatial distributions in mass concentrations and mass fractions of OS_i, OS_m, aliphatic OSs, aromatic OSs, and C_2–C_3 OSs in $PM_{2.5}$ collected in southern (KM and GZ) and northern (TY and XA) cities during winter. On average, OS_i was the dominant OS subgroup, which accounted for 37% – 46% and 68% – 69% of the total OS mass in southern and northern cities, respectively. The predominance of OS_i in aerosol OSs was also reported by previous studies in cities in northern (e.g., Beijing and Tianjin) (Wang et al. 2018; Ding et al. 2022) and southern (e.g., Guangzhou and Shanghai) (Wang et al. 2022; Wang et al. 2021) China, as well as in coastal (the Yellow Sea and Bohai Sea) (Wang et al. 2023) and European (Sweden) (Kanellopoulos et al. 2022) and American regions (Chen et al. 2021; Hettiyadura et al. 2017; Hettiyadura et al. 2019) (**Table S4**). Moreover, the concentrations of OS_i were significantly lower in southern cities (61 ± 38 ng m^{-3} – 87 ± 60 ng m^{-3}) than in northern cities (171 ± 69 ng m^{-3} – 260 ± 71 ng m^{-3}) (**Table S1**), showing a concentration range overlapped with previous observations (**Table S4**). From southern to northern cities, the mass concentrations and mass fractions of OS_m tended to decrease, which was opposite to the spatial variation pattern of OS_i (**Figure 1a**). Both OS_i and OS_m are generally considered as typical biogenic OSs (Hettiyadura et al. 2019; Wang et al. 2018), the abundances of which were tightly associated with biogenic VOC emissions when acidity, sulfate, atmospheric oxidation capacity, and ALW are not limiting factors (Bryant et al. 2021; Wang et al. 2022; Yang et al. 2024).

Thus, these dissimilarities in the spatial variations of OS_i and OS_m can be attributed to large differences in the intensity of biogenic VOC emissions (Wang et al. 2022) and/or the key factors that constrain OS formation between the northern and southern regions of China (**Table S1**).

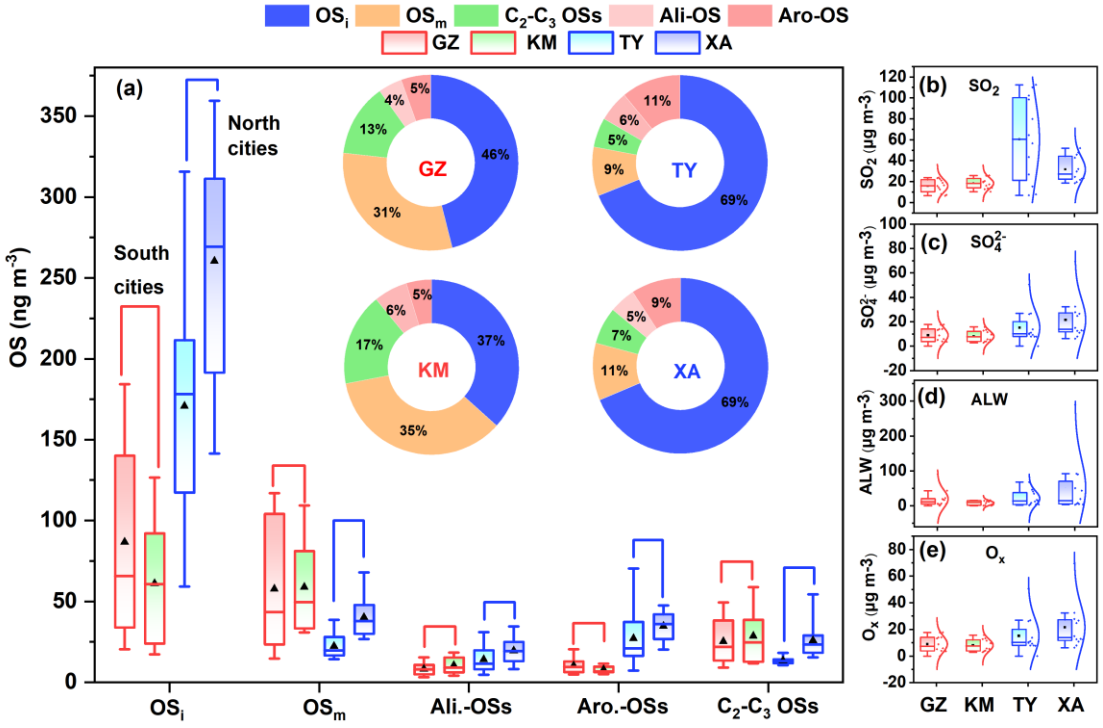

Figure 1 Box and whisker plots showing the variations in the concentration of different OS groups in $PM_{2.5}$ collected in southern (GZ and KM) and northern (TY and XA) cities of China during winter. Each box encompasses the 25th–75th percentiles. Whiskers are the minimum and maximum values. The triangles and solid lines inside boxes indicate the mean and median. The spatial variation in average percentage distributions of various OS groups was also shown in panel (a). The other figures show the spatial variations in (b) SO_2, (c)SO_4^{2-}, (d) ALW, and (e) O_x levels.

The abundance of anthropogenic OSs (i.e., OS_a, including aliphatic and aromatic

OSs, **Sect. S1**) in southern cities was lower than that of OS_m, which was opposite to the case in the northern cities showing higher anthropogenic OS abundance (**Figure 1a** and **Table S1**). Moreover, we found that the spatial variation patterns of OS_i and OS_a were similar to those of SO_2, SO_4^{2-}, ALW, and O_x (**Figures 1b–e**), as indicated by significant ($P < 0.05$) correlations of OS_i and OS_a with those factors (**Figure S3**). However, OS_m and C_2–C_3 OSs showed the opposite spatial variation pattern to SO_2, SO_4^{2-}, ALW, and O_x (**Figure 1**). If both OS_i and OS_m are assumed to be formed mainly from the oxidation of biologically emitted VOCs, the higher SO_2, SO_4^{2-}, ALW, and O_x levels could theoretically lead to higher OS_m in northern cities, just as these factors leaded to higher OS_i abundance in northern cities (**Figure 1** and **Table S1**). Accordingly, the above differentiated spatial variation patterns among different OS subgroups likely indicated that other sources of isoprene contributed to the formation of OS_i in northern cities. Further given the significant ($P < 0.05$) correlations between OS_i and OS_a, non biogenic isoprene emissions may play an important role in the formation of aerosol OS_i in northern cities. This will be further demonstrated in the following discussion.

3.2. Key factors affecting spatial differences in monoterpene-derived OS abundance

Figure 2a shows the distribution of OS_m concentration as a function of air temperature. We found that the OS_m concentration tended to increase with the increase of air temperature. Specifically, the air temperature in the southern cities was mainly

in the range of 7–14°C during the sampling period, corresponding to higher aerosol OS_m abundance. In contrast, the low temperature (< 7°C) in the northern cities corresponded to a significant decrease in OS_m abundance. This finding was similar to the previously observed decrease in aerosol OS_m compounds with decreasing temperature during winter in Guangzhou (Bryant et al. 2021). Furthermore, the indicator ($C_L \times C_T$) of biogenic VOC emission rate (Ding et al. 2016a; Guenther et al. 1993) was also higher in southern cities than in northern cities (**Figure 2b**), which implied higher monoterpene emissions in southern cities. It has been suggested that the emission rates of biogenic VOCs (e.g., monoterpene and isoprene) can be driven by increased air temperature and lighting (Ding et al. 2016a; Ding et al. 2016b). A previous study also found that the concentrations of atmospheric monoterpenes during the winter season were higher in warmer southern Chinese cities than in colder northern Chinese cities (Ding et al. 2016b; Li et al. 2020). In particular, GZ and KM, which encompass extensive areas of coniferous and broad-leaved forests, have been identified as hotspots for monoterpene and isoprene emissions (Li and Xie 2014). Considering the lower levels of key factors affecting OS formation observed in southern cities (**Figures 1b–e** and **Table S1**), it can be inferred that the significant spatial differences in OS_m abundances were largely attributed to temperature dependent emission of monoterpenes.

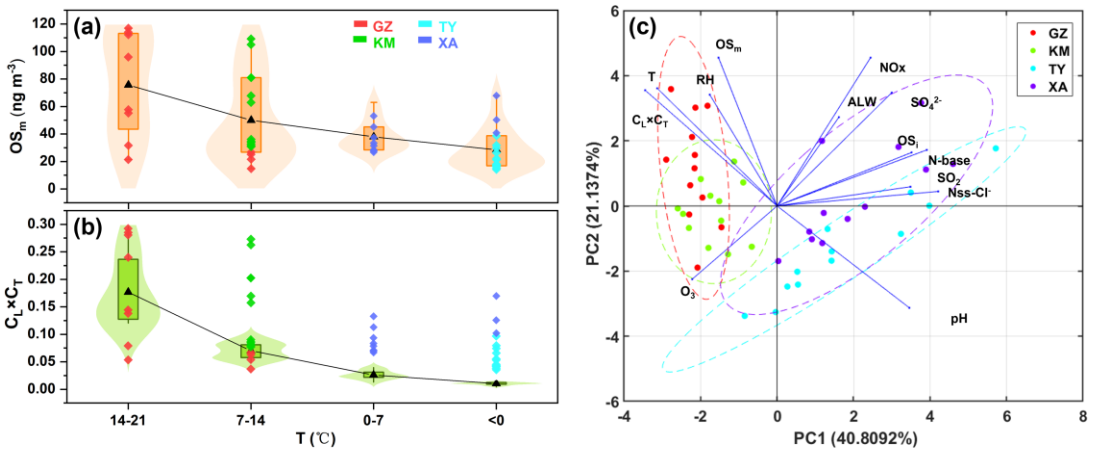

252

253 **Figure 2** Distribution of (a) OS_m and (b) $C_L \times C_T$ data in different temperature ranges
254 during winter. The triangles inside boxes indicate the mean. Principal component
255 analysis result (c) deciphering the relationship among OS_i, OS_m, and key factors
256 influencing OS formation.

257

258 To further determine the key factors affecting the spatial differences of OS_m,
259 principal component analysis was conducted (**Figure 2c**). It can be easily determined
260 that the abundance of aerosol OS_m was closely related to changes in air temperature
261 and $C_L \times C_T$ value. This further explained the changes in OS_m data in the southern
262 cities. In contrast, the abundance of aerosol OS_i in the northern cities was more
263 influenced by anthropogenic factors, as indicated by combustion source tracers such
264 as nitrogen-containing bases (N-bases) and non-sea-salt Cl^- (nss-Cl^-) (Wang et al.
265 2017; Jiang et al. 2023) (**Figure 2c**). Thus, principal component analysis can perfectly
266 distinguish the main factors causing changes in OS_m and OS_i abundances between the
267 northern and southern cities. In general, the above results confirm that the spatial
268 variation of OS_m was predominantly controlled by temperature-related monoterpene

emissions. However, this cannot account for the observed spatial variation of OS_i (**Figure 2c** and **Figure S4**). Interestingly, the spatial distribution patterns of OS_m and OS_i in northern and southern China exhibited consistency during summer, closely resembling the spatial distribution of biogenic VOC emission intensities (Wang et al. 2022). Thus, this case together with our observations during winter further imply that non biogenic sources of isoprene were important contributors to the formation of OS_i in northern China during winter.

3.3. Significant contribution of biomass burning to isoprene-derived OSs in Northern China

The previous principal component analysis has suggested that the abundance of OS_i in northern cities was closely related to the levels of combustion source tracers (e.g., N-base compounds and nss-Cl^-). N-base compounds are CHN species that contain exclusively C, H, and N atoms, and have been demonstrated to exhibit high sensitivity as molecular indicators in identifying biomass burning (Wang et al. 2017). To further confirm the potential contribution of combustion release to aerosol OS_i, OSs in smoke particles emitted from rice straw, pine branch, and coal combustion, as well as from gasoline vehicle exhausts, and diesel vehicle exhausts (**Figure S2**), were investigated. A total of 8 distinct OS_i were identified in both the smoke particles emitted from biomass burning (rice straw and pine branch) and the ambient aerosol particles, including $C_4H_7O_6S^-$, $C_5H_9O_6S^-$, $C_5H_{11}O_6S^-$, $C_5H_7O_7S^-$, $C_4H_7O_5S^-$, $C_5H_{11}O_7S^-$, $C_5H_9O_7S^-$, and $C_5H_9O_8S^-$. Moreover, the peak intensities of these 8 OS_i

in smoke particles emitted from fossil fuel combustion (gasoline and diesel vehicle exhausts and coal) were close to those in the blank sample. A previous investigation into CHOS compounds in smoke particles emitted from residential coal combustion and biomass burning also failed to identify OS_i species (Song et al. 2019; Song et al. 2018), which further supported the reliability of the combustion experiment conducted in this study. $C_5H_9O_6S^-$ was dominant OS_i species in pine-derived smoke particles (**Figure 3a,c**). We found that the average concentration of $C_5H_9O_6S^-$ in ambient aerosol samples was much higher in northern cities than in southern cities (**Figure 3b**). A reasonable explanation for this is that pine branches are commonly used as solid fuel for heating and cooking in northern suburbs and rural areas (Zhou et al. 2017). $C_5H_7O_7S^-$ and $C_4H_7O_5S^-$ dominated OS_i species in straw-derived smoke particles (**Figure 3a,c**). However, these two types of OS_i have relatively low abundance in ambient aerosol samples in both northern and southern cities. This may be attributed to the fact that straw burning was mainly concentrated in autumn rather than winter in China (Zhou et al. 2017; Yang et al. 2015). On average, the biomass burning-related OS_i accounted for 58% – 64% and 86% – 87% of the total OS_i concentration in southern and northern cities, respectively (**Figure 3c**). Although these biomass burning-related OS_i can also be formed through atmospheric transformation of biogenic isoprene, the higher proportion of these OS_i in northern cities together with previous principal component analysis results still support our previous consideration that non biogenic OS_i may be an important contributor to aerosol OS_i in northern cities.

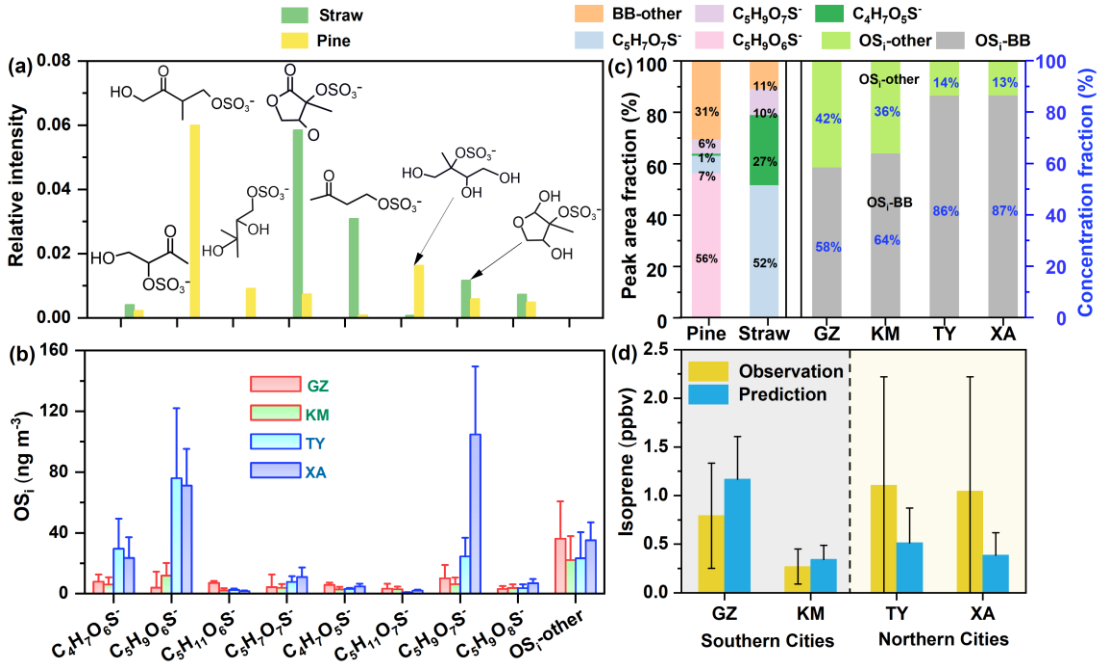

Figure 3 Relative signal intensity of (a) identified major OS_i species in different types of smoke particle samples. Spatial variation in the concentration of several specific OS_i (identified in smoke particles) in (b) ambient $PM_{2.5}$ samples. Peak area and concentration fraction of (c) OS_i species identified in both ambient $PM_{2.5}$ samples collected in different cities and smoke particles. Comparison of (d) isoprene mixing ratios obtained from observation and modeling in different cities (Zhang et al. 2020).

Previous laboratory studies have suggested that these identified OS_i species in biomass burning-derived smoke particles are typically formed through heterogeneous and multiphase reactions involving isoprene, its oxidation intermediates, and sulfate or sulfur dioxide (Surratt et al. 2008; Surratt et al. 2007; Darer et al. 2011). Specifically, $C_5H_9O_6S^-$, as a sulfate ester of C_5-alkene triols, was formed mainly through the uptake of gas-phase isoprene oxidation products onto acidified sulfate aerosol (Surratt et al. 2007). The formation of $C_5H_7O_7S^-$ and $C_5H_9O_7S^-$ begins with

the gas-phase oxidation of isoprene (Surratt et al. 2008). $C_4H_7O_6S^-$ can be generated both from isoprene photooxidation and sulfate radical reaction with methacrolein (MACR) or methyl vinyl ketone (MVK) (Schindelka et al. 2013; Wach et al. 2019; Nozière et al. 2010). $C_5H_{11}O_7S^-$ was produced by reactive uptake of isoprene-derived epoxide (IEPOX) on sulfate under low-NOx conditions. Since our combustion experiments have excluded the direct contribution of ambient aerosol particles to OS_i in smoke particles, it can be expected that these detected OS_i compounds were mainly generated within smoke plumes through the isoprene oxidation pathway mentioned above. It has been demonstrated that directly emitted organic aerosols or VOCs can undergo a chemical reaction within smoke plumes, forming secondary organic compounds within a matter of hours (Wang et al. 2017; Song et al. 2018; Mason et al. 2001). A field study conducted by Zhu et al. (2016) at a rural site (Yucheng) in the North China Plain (NCP) region has observed that the concentration of ambient isoprene during the period of straw combustion was approximately twice as high as that observed during periods of non combustion. In addition, Li et al. (2018) found that isoprene-derived epoxides increased significantly during field open burning of straw. Generally, despite the fact that a few of the mechanisms by which OSs are formed have been verified through field studies, the formation of CHOS and CHONS compounds has been observed to occur in the biomass burning plume (Zhang et al. 2024; Song et al. 2018; Tang et al. 2020). Thus, these previous case studies further support our consideration that OS_i compounds formed in biomass burning-derived smoke particles in this study can be attributed to increasing isoprene emission caused

by field biomass burning (Zhu et al. 2016) and favorable aqueous secondary organic aerosols (SOA) formation during the aging process of the biomass burning plume (Gilardoni et al. 2016).

Figure 3d presents a comparison between the isoprene mixing ratios derived from model simulations (plant functional type related model) and those observed in the field in different Chinese cities during winter (December and January) (Zhang et al. 2020). Overall, the levels of isoprene observed in northern cities during winter were higher than those in southern cities. In addition, the predicted values in southern cities were slightly higher than the observed values, which may be attributed to the lag in model prediction results caused by the rapid urbanization rates in these southern cities (Zhang et al. 2020). However, the observed values in these two northern cities were 53% to 63% higher than the predicted values, on average. Clearly, this plant functional type related isoprene prediction model cannot explain the large amount of "missing" isoprene sources in northern cities. Thus, the observed spatial differences in OS_i (**Figure 1**) and field combustion experiments (**Figure 3**) can suggest that these "missing" isoprene sources were mainly derived from biomass burning, significantly contributing to the production of aerosol OS_i in northern cities. This can also be supported by previous principal component analysis involving combustion source tracers and OS_i compounds (**Figure 2c**).

3.4. Formation of anthropogenic OSs mainly driven by fossil fuel and biomass combustion

Figures 4a,b show the average concentration distribution of anthropogenic OSs classified based on the number of O atoms in their molecules in southern (GZ and KM) and northern (TY and XA) cities. The O_4S_1 subgroup was the most abundant aromatic OSs in both southern and northern cities, among which $C_9H_9O_4S^-$, phenyl sulfate ($C_6H_5O_4S^-$), and benzyl sulfate ($C_7H_7O_4S^-$) were dominant species (**Table S3**). $C_7H_7O_4S^-$ and $C_6H_5O_4S^-$ have been suggested to be formed mainly through the photooxidation of 2-methylnaphthalene and naphthalene (Riva et al. 2015), or alternatively, by the sulfate radical reaction with aromatic compounds, including toluene and benzoic acid, in an aqueous phase environment (Riva et al. 2015). The formation mechanism of $C_9H_9O_4S^-$ is rarely reported. However, $C_9H_9O_4S^-$, $C_6H_5O_4S^-$, and $C_7H_7O_4S^-$ were also detected in both fossil fuel combustion-derived smoke particles and biomass burning-derived smoke particles (**Figure S5** and **Table S5**), indicating that the aromatic VOCs produced by fuel combustion are closely related to the formation of these aromatic OSs. Overall, aerosol aromatic OS compounds in both southern and northern cities were mainly distributed between four and six O atoms (**Figure 4c**), which was similar to the distribution of aromatic OSs identified in various smoke particles emitted from different combustion sources (**Figure 4d**). However, the average abundances of aromatic $O_{4–6}S_1$ compounds in northern cities were 3–6 times higher than those in southern cities. The above results suggest that aromatic OSs originated from fossil fuel and biomass combustion activities are important contributors to urban aerosol anthropogenic OSs in winter in China, especially in northern cities. We found that the correlations between aromatic OSs and

anthropogenic indicators (SO_2, SO_4^{2-}, N-base, and nss-Cl^-) were stronger in northern cities than in southern cities (**Figure S6**), and that the release of polycyclic aromatic hydrocarbons from fossil fuel combustion was also higher in northern cities (**Figure S7**). This further indicates that higher aerosol aromatic OSs in northern cities was mainly attributed to stronger combustion activities in those cities.

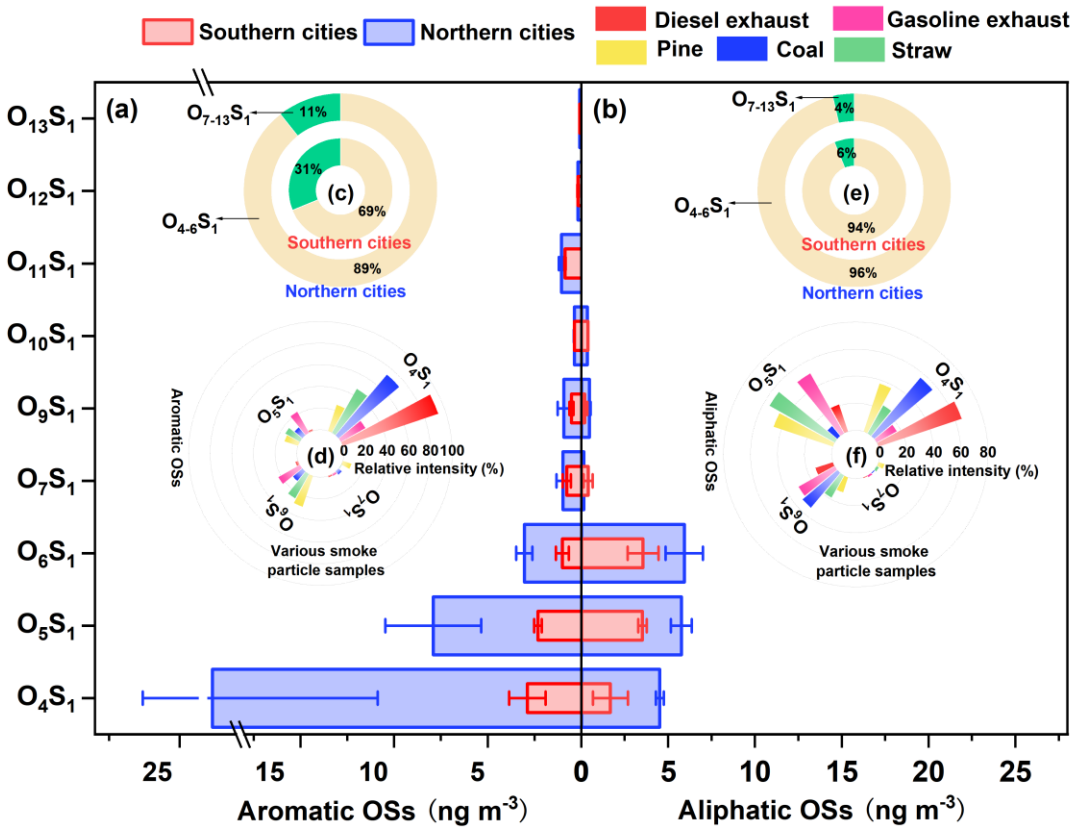

Figure 4 Concentration distribution of different (a) aromatic and (b) aliphatic OS subgroups (classification based on oxygen atoms) in southern and northern cities. Ring charts (c,e) show the percentage contributions of $O_{4\text{-}6}S_1$ and $O_{7\text{-}13}S_1$ subgroups. Radial bar charts (d,f) illustrate the relative signal intensity of different OS subgroups in different smoke particle samples.

Aliphatic OSs were also predominantly distributed between O_4S_1 and O_6S_1

subgroups in both southern and northern cities (**Figures 4b,e**), which was similar to the case found in both fossil fuel combustion-derived smoke particles and biomass burning-derived smoke particles (**Figure 4f**). It has been suggested that the long-chain alkanes derived from traffic emissions can largely contribute to the formation of CHOS compounds with aliphatic carbon chains (Tao et al. 2014). In addition, Tang et al. (2020) analyzed the molecular compositions of smoke particles from open biomass burning, household coal combustion and vehicle emissions and suggested that the aliphatic CHOS compounds can be derived from both vehicle emissions and coal and biomass combustion. In this study, aliphatic OSs showed a significant ($P < 0.05$) positive correlation with nss-Cl^-, SO_2, NO_x, and N-base compounds in both southern and northern cities (**Figure S6** and **S8**), indicating aerosol aliphatic OSs were affected by a combination of biomass burning and vehicle emissions in those cities during winter. Thus, the significantly higher level of aliphatic $O_{4-6}S_1$ species in northern cities indicated that the formation of aliphatic OSs in northern cities was more driven by pollutants released from the combustion of fossil fuels and biomass compared to southern cities. This consideration is highly consistent with the fact that the concentrations of air pollutants (e.g., SO_2 and NO_2) in northern cities with a large demand for heating during winter are usually higher than those in warmer southern cities (**Table S1** and **Figure S1b**) (Yu et al. 2020; Ding et al. 2017; Ma et al. 2017; Zhou et al. 2017).

4. Conclusion and atmospheric implications

It has been previously suggested that isoprene can also be released into the atmosphere as a result of open burning of agricultural residues and forest fires (Andreae 2019; Simpson et al. 2011). A field study conducted by (Wang et al. 2019) in Beijing during winter inferred that the prevalence of OS_i compounds in total aerosol OSs may be partially attributable to biomass burning emissions, although there was a paucity of compelling evidence to support this hypothesis. This work combines strongly contrasting observational studies (northern Chinese Cities vs southern Chinese Cities) with in situ combustion modelling experiments to provide the first direct evidence that biomass burning emission, rather than fossil fuel combustion emission, is a significant contributor to aerosol OS_i in northern cities (**Figure 5**). In Chinese cities, particularly those in the northern region, biomass materials are extensively utilized for domestic heating and cooking purposes during the winter season (Zhou et al. 2017). Clearly, the isoprene emissions from biomass combustion sources would result in higher isoprene mixing ratios than those simulated by the model (Zhang et al. 2020) that only considers natural isoprene emissions. Thus, isoprene prediction models applied to Chinese winters in the future should also take into account the various biomass combustion source releases. Given the potential for both biomass burning and biogenic isoprene to contribute to OS_i formation, separating their respective contributions remains challenging. Furthermore, biogenic OSs are important SOA constituents and have been frequently serve as important tracers for biogenic SOA (Ding et al. 2014; Ding et al. 2016a). The overall results suggest that some OS_i species may not be suitable as biogenic SOA markers,

451 especially in areas with intensive biomass burning activities, such as northern Chinese
452 cities during winter.
453

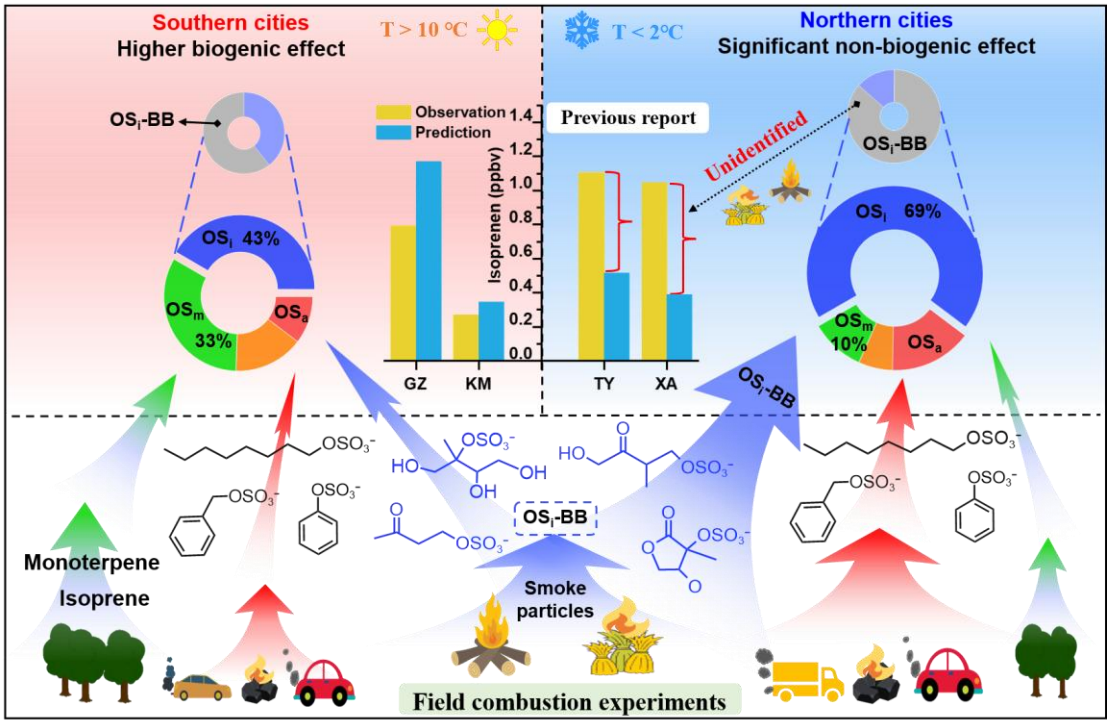

454

455 **Figure 5** Conceptual picture showing the characteristics and main contributors of OSs
456 in northern and southern China during winter. It is noteworthy that OS_i-BB can
457 originate not only from biomass combustion, but also from the secondary formation
458 of isoprene emitted from biogenic sources.
459

460 We found that different fossil fuel combustion emissions (e.g., vehicle emissions
461 and coal combustion emissions) and biomass burning emissions can contribute to
462 aerosol anthropogenic OSs. However, current studies have not been able to accurately
463 distinguish between the contributions of various material combustion to different
464 types of anthropogenic OSs. Future research is necessary to develop more

comprehensive models to further explore the effects of various combustion sources on the generation and reduction of urban aerosol OS pollution. Of particular importance is that although the production of various OSs was directly observed through our simulated combustion experiments, it is not clear whether the chemical mechanisms involved are similar to those derived from the laboratory simulations. This is because the combustion process is accompanied by the effects of high temperatures. In general, although our results provide direct evidence for the release of OSs from combustion of various combustion sources, further mechanistic studies and environmental impact assessment are still urgently needed. This may be important for effective control of urban wintertime organic aerosol pollution in China.

Data availability

The data presented in this work are available upon request from the corresponding authors.

Competing interests

The authors declare no conflicts of interest relevant to this study.

Author contributions

YX designed the study. TY, YJM, HWX, and HX performed field measurements and sample collection; TY and YJM performed chemical analysis; YX and TY performed data analysis; YX and TY wrote the original manuscript; and YX, TY, YCW, and

HYX reviewed and edited the manuscript.

Acknowledgements

The authors are very grateful to Jian-Zhen Yu at the Hong Kong University of Science and Technology for her kind and valuable comments to improve the paper.

Financial support

This study was kindly supported by the National Natural Science Foundation of China (grant number 42303081, 42373083, and 22306059), the Shanghai "Science and Technology Innovation Action Plan" Shanghai Sailing Program (grant number 22YF1418700), and the National Key Research and Development Program of China (grant number 2023YFF0806001).

References

Andreae, M. O.: Emission of trace gases and aerosols from biomass burning – an updated assessment, Atmos. Chem. Phys., 19, 8523-8546, 10.5194/acp-19-8523-2019, 2019.

Aoki, E., Sarrimanolis, J. N., Lyon, S. A., and Elrod, M. J.: Determining the Relative Reactivity of Sulfate, Bisulfate, and Organosulfates with Epoxides on Secondary Organic Aerosol, ACS Earth Space Chem., 4, 1793-1801, 10.1021/acsearthspacechem.0c00178, 2020.

Brüggemann, M., Riva, M., Perrier, S., Poulain, L., George, C., and Herrmann, H.: Overestimation of Monoterpene Organosulfate Abundance in Aerosol Particles by Sampling in the Presence of SO2, Environ. Sci. Technol. Lett., 8, 206-211, 10.1021/acs.estlett.0c00814, 2020a.

Brüggemann, M., Xu, R., Tilgner, A., Kwong, K. C., Mutzel, A., Poon, H. Y., Otto, T., Schaefer, T., Poulain, L., Chan, M. N., and Herrmann, H.: Organosulfates in Ambient Aerosol: State of Knowledge and Future Research Directions on Formation, Abundance, Fate, and Importance, Environ. Sci. Technol., 54, 3767-3782, 10.1021/acs.est.9b06751, 2020b.

Bryant, D. J., Elzein, A., Newland, M., White, E., Swift, S., Watkins, A., Deng, W., Song, W., Wang, S., Zhang, Y., Wang, X., Rickard, A. R., and Hamilton, J. F.: Importance of Oxidants and Temperature in the Formation of Biogenic Organosulfates and Nitrooxy Organosulfates, ACS Earth Space Chem., 5, 2291-2306, 10.1021/acsearthspacechem.1c00204, 2021.

Chen, Y., Dombek, T., Hand, J., Zhang, Z., Gold, A., Ault, A. P., Levine, K. E., and Surratt, J. D.: Seasonal Contribution of Isoprene-Derived Organosulfates to Total Water-Soluble Fine Particulate Organic Sulfur in the United States, ACS Earth Space Chem., 5, 2419-2432, 10.1021/acsearthspacechem.1c00102, 2021.

Cui, T., Zeng, Z., dos Santos, E. O., Zhang, Z., Chen, Y., Zhang, Y., Rose, C. A., Budisulistiorini, S. H.,

524 Collins, L. B., Bodnar, W. M., de Souza, R. A. F., Martin, S. T., Machado, C. M. D., Turpin, B. J.,
525 Gold, A., Ault, A. P., and Surratt, J. D.: Development of a hydrophilic interaction liquid
526 chromatography (HILIC) method for the chemical characterization of water-soluble isoprene
527 epoxydiol (IEPOX)-derived secondary organic aerosol, Environ. Sci.: Process. Impacts, 20, 1524-
528 1536, 10.1039/c8em00308d, 2018.
529 Darer, A. I., Cole-Filipiak, N. C., O'Connor, A. E., and Elrod, M. J.: Formation and Stability of
530 Atmospherically Relevant Isoprene-Derived Organosulfates and Organonitrates, Environ. Sci.
531 Technol., 45, 1895-1902, 10.1021/es103797z, 2011.
532 Ding, S., Chen, Y., Devineni, S. R., Pavuluri, C. M., and Li, X.-D.: Distribution characteristics of
533 organosulfates (OSs) in PM2.5 in Tianjin, Northern China: Quantitative analysis of total and three
534 OS species, Sci. Total Environ., 834, 10.1016/j.scitotenv.2022.155314, 2022.
535 Ding, X., He, Q.-F., Shen, R.-Q., Yu, Q.-Q., and Wang, X.-M.: Spatial distributions of secondary
536 organic aerosols from isoprene, monoterpenes,β-caryophyllene, and aromatics over China during
537 summer, J. Geophys. Res. Atmos., 119, 11,877-811,891, 10.1002/2014jd021748, 2014.
538 Ding, X., He, Q.-F., Shen, R.-Q., Yu, Q.-Q., Zhang, Y.-Q., Xin, J.-Y., Wen, T.-X., and Wang, X.-M.:
539 Spatial and seasonal variations of isoprene secondary organic aerosol in China: Significant impact
540 of biomass burning during winter, Sci. Rep., 6, 10.1038/srep20411, 2016a.
541 Ding, X., Zhang, Y.-Q., He, Q.-F., Yu, Q.-Q., Wang, J.-Q., Shen, R.-Q., Song, W., Wang, Y.-S., and
542 Wang, X.-M.: Significant Increase of Aromatics-Derived Secondary Organic Aerosol during Fall
543 to Winter in China, Environ. Sci. Technol., 51, 7432-7441, 10.1021/acs.est.6b06408, 2017.
544 Ding, X., Zhang, Y. Q., He, Q. F., Yu, Q. Q., Shen, R. Q., Zhang, Y., Zhang, Z., Lyu, S. J., Hu, Q. H.,
545 Wang, Y. S., Li, L. F., Song, W., and Wang, X. M.: Spatial and seasonal variations of secondary

organic aerosol from terpenoids over China, J. Geophys. Res. Atmos., 121, 10.1002/2016jd025467, 2016b.

Duporté, G., Flaud, P. M., Geneste, E., Augagneur, S., Pangui, E., Lamkaddam, H., Gratien, A., Doussin, J. F., Budzinski, H., Villenave, E., and Perraudin, E.: Experimental Study of the Formation of Organosulfates from α-Pinene Oxidation. Part I: Product Identification, Formation Mechanisms and Effect of Relative Humidity, J. Phys. Chem. A, 120, 7909-7923, 10.1021/acs.jpca.6b08504, 2016.

Duporté, G., Flaud, P. M., Kammer, J., Geneste, E., Augagneur, S., Pangui, E., Lamkaddam, H., Gratien, A., Doussin, J. F., Budzinski, H., Villenave, E., and Perraudin, E.: Experimental Study of the Formation of Organosulfates from α-Pinene Oxidation. 2. Time Evolution and Effect of Particle Acidity, J. Phys. Chem. A, 124, 409-421, 10.1021/acs.jpca.9b07156, 2019.

Fleming, L. T., Ali, N. N., Blair, S. L., Roveretto, M., George, C., and Nizkorodov, S. A.: Formation of Light-Absorbing Organosulfates during Evaporation of Secondary Organic Material Extracts in the Presence of Sulfuric Acid, ACS Earth Space Chem., 3, 947-957, 10.1021/acsearthspacechem.9b00036, 2019.

Gilardoni, S., Massoli, P., Paglione, M., Giulianelli, L., Carbone, C., Rinaldi, M., Decesari, S., Sandrini, S., Costabile, F., Gobbi, G. P., Pietrogrande, M. C., Visentin, M., Scotto, F., Fuzzi, S., and Facchini, M. C.: Direct observation of aqueous secondary organic aerosol from biomass-burning emissions, Proc. Natl. Acad. Sci. U.S.A., 113, 10013-10018, 10.1073/pnas.1602212113, 2016.

Guenther, A. B., Zimmerman, P. R., Harley, P. C., Monson, R. K., and Fall, R.: Isoprene and monoterpene emission rate variability J. Geophys. Res. Atmos., 98, 12609-12617, 1993.

He, L. Y., Lin, Y., Huang, X. F., Guo, S., Xue, L., Su, Q., Hu, M., Luan, S. J., and Zhang, Y. H.: Characterization of high-resolution aerosol mass spectra of primary organic aerosol emissions from Chinese cooking and biomass burning, Atmos. Chem. Phys., 10, 11535-11543, 10.5194/acp-10-11535-2010, 2010.

Hettiyadura, A. P. S., Al-Naiema, I. M., Hughes, D. D., Fang, T., and Stone, E. A.: Organosulfates in Atlanta, Georgia: anthropogenic influences on biogenic secondary organic aerosol formation, Atmos. Chem. Phys., 19, 3191-3206, 10.5194/acp-19-3191-2019, 2019.

Hettiyadura, A. P. S., Stone, E. A., Kundu, S., Baker, Z., Geddes, E., Richards, K., and Humphry, T.: Determination of atmospheric organosulfates using HILIC chromatography with MS detection, Atmos. Meas. Tech., 8, 2347-2358, 10.5194/amt-8-2347-2015, 2015.

Hettiyadura, A. P. S., Jayarathne, T., Baumann, K., Goldstein, A. H., de Gouw, J. A., Koss, A., Keutsch, F. N., Skog, K., and Stone, E. A.: Qualitative and quantitative analysis of atmospheric organosulfates in Centreville, Alabama, Atmos. Chem. Phys., 17, 1343-1359, 10.5194/acp-17-1343-2017, 2017.

Huang, L., Wang, Y., Zhao, Y., Hu, H., Yang, Y., Wang, Y., Yu, J. Z., Chen, T., Cheng, Z., Li, C., Li, Z., and Xiao, H.: Biogenic and Anthropogenic Contributions to Atmospheric Organosulfates in a Typical Megacity in Eastern China, J. Geophys. Res. Atmos., 128, 10.1029/2023jd038848, 2023.

Jiang, H., Cai, J., Feng, X., Chen, Y., Wang, L., Jiang, B., Liao, Y., Li, J., Zhang, G., Mu, Y., and Chen, J.: Aqueous-Phase Reactions of Anthropogenic Emissions Lead to the High Chemodiversity of Atmospheric Nitrogen-Containing Compounds during the Haze Event, Environ. Sci. Technol., 57, 16500-16511, 10.1021/acs.est.3c06648, 2023.

Kanellopoulos, P. G., Kotsaki, S. P., Chrysochou, E., Koukoulakis, K., Zacharopoulos, N.,

590 Philippopoulos, A., and Bakeas, E.: PM2.5-bound organosulfates in two Eastern Mediterranean
591 cities: The dominance of isoprene organosulfates, Chemosphere, 297,
592 10.1016/j.chemosphere.2022.134103, 2022.
593 Kristensen, K., Bilde, M., Aalto, P. P., Petäjä, T., and Glasius, M.: Denuder/filter sampling of organic
594 acids and organosulfates at urban and boreal forest sites: Gas/particle distribution and possible
595 sampling artifacts, Atmos. Environ., 130, 36-53, 10.1016/j.atmosenv.2015.10.046, 2016.
596 Li, J., Wang, G., Wu, C., Cao, C., Ren, Y., Wang, J., Li, J., Cao, J., Zeng, L., and Zhu, T.:
597 Characterization of isoprene-derived secondary organic aerosols at a rural site in North China
598 Plain with implications for anthropogenic pollution effects, Sci. Rep., 8, 10.1038/s41598-017-
599 18983-7, 2018.
600 Li, L., Yang, W., Xie, S., and Wu, Y.: Estimations and uncertainty of biogenic volatile organic
601 compound emission inventory in China for 2008–2018, Sci. Total Environ., 733,
602 10.1016/j.scitotenv.2020.139301, 2020.
603 Li, L. Y. and Xie, S. D.: Historical variations of biogenic volatile organic compound emission
604 inventories in China, 1981–2003, Atmos. Environ., 95, 185-196, 10.1016/j.atmosenv.2014.06.033,
605 2014.
606 Lin, X., Xu, Y., Zhu, R. G., Xiao, H. W., and Xiao, H. Y.: Proteinaceous Matter in PM2.5 in Suburban
607 Guiyang, Southwestern China: Decreased Importance in Long-Range Transport and Atmospheric
608 Degradation, J. Geophys. Res. Atmos., 128, 10.1029/2023jd038516, 2023.
609 Liu, T., Xu, Y., Sun, Q. B., Xiao, H. W., Zhu, R. G., Li, C. X., Li, Z. Y., Zhang, K. Q., Sun, C. X., and
610 Xiao, H. Y.: Characteristics, Origins, and Atmospheric Processes of Amines in Fine Aerosol
611 Particles in Winter in China, J. Geophys. Res. Atmos., 128, 10.1029/2023jd038974, 2023.

612 Luk´acs, H., Gelencs´er, A., Hoffer, A., Kiss, G., Horv´ath, K., and Harty´ani, Z.: Quantitative
613 assessment of organosulfates in size-segregated rural fine aerosol, Atmos. Chem. Phys., 9, 231-
614 238, 10.5194/acp-9-231-2009, 2009.
615 Ma, Q., Cai, S., Wang, S., Zhao, B., Martin, R. V., Brauer, M., Cohen, A., Jiang, J., Zhou, W., Hao, J.,
616 Frostad, J., Forouzanfar, M. H., and Burnett, R. T.: Impacts of coal burning on ambient PM2.5
617 pollution in China, Atmos. Chem. Phys., 17, 4477-4491, 10.5194/acp-17-4477-2017, 2017.
618 Mason, S. A., Field, R. J., Yokelson, R. J., Kochivar, M. A., Tinsley, M. R., Ward, D. E., and Hao, W.
619 M.: Complex effects arising in smoke plume simulations due to inclusion of direct emissions of
620 oxygenated organic species from biomass combustion, J. Geophys. Res. Atmos., 106, 12527-
621 12539, 10.1029/2001jd900003, 2001.
622 Nozière, B., Ekström, S., Alsberg, T., and Holmström, S.: Radical-initiated formation of organosulfates
623 and surfactants in atmospheric aerosols, Geophys. Res. Lett., 37, n/a-n/a, 10.1029/2009gl041683,
624 2010.
625 Riva, M., Tomaz, S., Cui, T., Lin, Y.-H., Perraudin, E., Gold, A., Stone, E. A., Villenave, E., and
626 Surratt, J. D.: Evidence for an Unrecognized Secondary Anthropogenic Source of Organosulfates
627 and Sulfonates: Gas-Phase Oxidation of Polycyclic Aromatic Hydrocarbons in the Presence of
628 Sulfate Aerosol, Environ. Sci. Technol., 49, 6654-6664, 10.1021/acs.est.5b00836, 2015.
629 Riva, M., Chen, Y., Zhang, Y., Lei, Z., Olson, N. E., Boyer, H. C., Narayan, S., Yee, L. D., Green, H. S.,
630 Cui, T., Zhang, Z., Baumann, K., Fort, M., Edgerton, E., Budisulistiorini, S. H., Rose, C. A.,
631 Ribeiro, I. O., e Oliveira, R. L., dos Santos, E. O., Machado, C. M. D., Szopa, S., Zhao, Y., Alves,
632 E. G., de Sá, S. S., Hu, W., Knipping, E. M., Shaw, S. L., Duvoisin Junior, S., de Souza, R. A. F.,
633 Palm, B. B., Jimenez, J.-L., Glasius, M., Goldstein, A. H., Pye, H. O. T., Gold, A., Turpin, B. J.,

Vizuete, W., Martin, S. T., Thornton, J. A., Dutcher, C. S., Ault, A. P., and Surratt, J. D.: Increasing Isoprene Epoxydiol-to-Inorganic Sulfate Aerosol Ratio Results in Extensive Conversion of Inorganic Sulfate to Organosulfur Forms: Implications for Aerosol Physicochemical Properties, Environ. Sci. Technol., 53, 8682-8694, 10.1021/acs.est.9b01019, 2019.

Schindelka, J., Iinuma, Y., Hoffmann, D., and Herrmann, H.: Sulfate radical-initiated formation of isoprene-derived organosulfates in atmospheric aerosols, Faraday Discuss., 165, 10.1039/c3fd00042g, 2013.

Simpson, I. J., Akagi, S. K., Barletta, B., Blake, N. J., Choi, Y., Diskin, G. S., Fried, A., Fuelberg, H. E., Meinardi, S., Rowland, F. S., Vay, S. A., Weinheimer, A. J., Wennberg, P. O., Wiebring, P., Wisthaler, A., Yang, M., Yokelson, R. J., and Blake, D. R.: Boreal forest fire emissions in fresh Canadian smoke plumes: C_1-C_{10} volatile organic compounds (VOCs), CO_2, CO, NO_2, NO, HCN and CH_3CN, Atmos. Chem. Phys., 11, 6445-6463, 10.5194/acp-11-6445-2011, 2011.

Song, J., Li, M., Jiang, B., Wei, S., Fan, X., and Peng, P. a.: Molecular Characterization of Water-Soluble Humic like Substances in Smoke Particles Emitted from Combustion of Biomass Materials and Coal Using Ultrahigh-Resolution Electrospray Ionization Fourier Transform Ion Cyclotron Resonance Mass Spectrometry, Environ. Sci. Technol., 52, 2575-2585, 10.1021/acs.est.7b06126, 2018.

Song, J., Li, M., Fan, X., Zou, C., Zhu, M., Jiang, B., Yu, Z., Jia, W., Liao, Y., and Peng, P. a.: Molecular Characterization of Water- and Methanol-Soluble Organic Compounds Emitted from Residential Coal Combustion Using Ultrahigh-Resolution Electrospray Ionization Fourier Transform Ion Cyclotron Resonance Mass Spectrometry, Environ. Sci. Technol., 53, 13607-13617, 10.1021/acs.est.9b04331, 2019.

656 Surratt, J. D., Kroll, J. H., Kleindienst, T. E., Edney, E. O., Claeys, M., Sorooshian, A., Ng, L.,
657 Offenberg, J. H., Lewandowski, M., Jaoui, M., Flagan, R. C., and Seinfeld, J. H.: Evidence for
658 organosulfates in secondary organic aerosol., Environ. Sci. Technol., 41, 517-527, 2007.
659 Surratt, J. D., Gómez-González, Y., Chan, A. W., Vermeylen, R., Shahgholi, M., Kleindienst, T. E.,
660 Edney, E. O., Offenberg, J. H., Lewandowski, M., Jaoui, M., Maenhaut, M. W., Claeys, M.,
661 Flagan, R. C., and Seinfeld, J. H.: Organosulfate Formation in Biogenic Secondary Organic
662 Aerosol, J. Phys. Chem. A, 112, 8345-8378, 2008.
663 Tang, J., Li, J., Su, T., Han, Y., Mo, Y., Jiang, H., Cui, M., Jiang, B., Chen, Y., Tang, J., Song, J., Peng,
664 P. a., and Zhang, G.: Molecular compositions and optical properties of dissolved brown carbon in
665 biomass burning, coal combustion, and vehicle emission aerosols illuminated by excitation–
666 emission matrix spectroscopy and Fourier transform ion cyclotron resonance mass spectrometry
667 analysis, Atmos. Chem. Phys., 20, 2513-2532, 10.5194/acp-20-2513-2020, 2020.
668 Tao, S., Lu, X., Levac, N., Bateman, A. P., Nguyen, T. B., Bones, D. L., Nizkorodov, S. A., Laskin, J.,
669 Laskin, A., and Yang, X.: Molecular Characterization of Organosulfates in Organic Aerosols from
670 Shanghai and Los Angeles Urban Areas by Nanospray-Desorption Electrospray Ionization High-
671 Resolution Mass Spectrometry, Environ. Sci. Technol., 48, 10993-11001, 10.1021/es5024674,
672 2014.
673 Wach, P., Spólnik, G., Rudziński, K. J., Skotak, K., Claeys, M., Danikiewicz, W., and Szmigielski, R.:
674 Radical oxidation of methyl vinyl ketone and methacrolein in aqueous droplets: Characterization
675 of organosulfates and atmospheric implications, Chemosphere, 214, 1-9,
676 10.1016/j.chemosphere.2018.09.026, 2019.
677 Wang, K., Zhang, Y., Huang, R.-J., Wang, M., Ni, H., Kampf, C. J., Cheng, Y., Bilde, M., Glasius, M.,

678 and Hoffmann, T.: Molecular Characterization and Source Identification of Atmospheric
679 Particulate Organosulfates Using Ultrahigh Resolution Mass Spectrometry, Environ. Sci. Technol.,
680 53, 6192-6202, 10.1021/acs.est.9b02628, 2019.
681 Wang, Y., Ma, Y., Kuang, B., Lin, P., Liang, Y., Huang, C., and Yu, J. Z.: Abundance of organosulfates
682 derived from biogenic volatile organic compounds: Seasonal and spatial contrasts at four sites in
683 China, Sci. Total Environ., 806, 10.1016/j.scitotenv.2021.151275, 2022.
684 Wang, Y., Zhao, Y., Wang, Y., Yu, J.-Z., Shao, J., Liu, P., Zhu, W., Cheng, Z., Li, Z., Yan, N., and Xiao,
685 H.: Organosulfates in atmospheric aerosols in Shanghai, China: seasonal and interannual
686 variability, origin, and formation mechanisms, Atmos. Chem. Phys., 21, 2959-2980, 10.5194/acp-
687 21-2959-2021, 2021.
688 Wang, Y., Hu, M., Wang, Y.-C., Li, X., Fang, X., Tang, R., Lu, S., Wu, Y., Guo, S., Wu, Z., Hallquist,
689 M., and Yu, J. Z.: Comparative Study of Particulate Organosulfates in Contrasting Atmospheric
690 Environments: Field Evidence for the Significant Influence of Anthropogenic Sulfate and NOx,
691 Environ. Sci. Technol. Lett., 7, 787-794, 10.1021/acs.estlett.0c00550, 2020.
692 Wang, Y., Hu, M., Lin, P., Guo, Q., Wu, Z., Li, M., Zeng, L., Song, Y., Zeng, L., Wu, Y., Guo, S.,
693 Huang, X., and He, L.: Molecular Characterization of Nitrogen-Containing Organic Compounds
694 in Humic-like Substances Emitted from Straw Residue Burning, Environ. Sci. Technol., 51, 5951-
695 5961, 10.1021/acs.est.7b00248, 2017.
696 Wang, Y., Zhang, Y., Li, W., Wu, G., Qi, Y., Li, S., Zhu, W., Yu, J. Z., Yu, X., Zhang, H.-H., Sun, J.,
697 Wang, W., Sheng, L., Yao, X., Gao, H., Huang, C., Ma, Y., and Zhou, Y.: Important Roles and
698 Formation of Atmospheric Organosulfates in Marine Organic Aerosols: Influence of
699 Phytoplankton Emissions and Anthropogenic Pollutants, Environ. Sci. Technol., 57, 10284-10294,

10.1021/acs.est.3c01422, 2023.

Wang, Y., Hu, M., Guo, S., Wang, Y., Zheng, J., Yang, Y., Zhu, W., Tang, R., Li, X., Liu, Y., Le Breton, M., Du, Z., Shang, D., Wu, Y., Wu, Z., Song, Y., Lou, S., Hallquist, M., and Yu, J.: The secondary formation of organosulfates under interactions between biogenic emissions and anthropogenic pollutants in summer in Beijing, Atmos. Chem. Phys., 18, 10693-10713, 10.5194/acp-18-10693-2018, 2018.

Xu, J., Shen, G., Fu, B., Han, Y., Suo, X., Chen, Z., Lai, Y., Li, J., Li, L., Han, L., Tao, S., and Li, B.: Emissions of Particulate and Previously Ignored Gaseous Phosphorus from Coal and Biomass Combustion in Household Stoves, Environ. Sci. Technol. Lett., 10, 1011-1016, 10.1021/acs.estlett.3c00029, 2023a.

Xu, Y., Dong, X. N., Xiao, H. Y., Zhou, J. X., and Wu, D. S.: Proteinaceous Matter and Liquid Water in Fine Aerosols in Nanchang, Eastern China: Seasonal Variations, Sources, and Potential Connections, J. Geophys. Res. Atmos., 127, 10.1029/2022jd036589, 2022.

Xu, Y., Dong, X.-N., He, C., Wu, D.-S., Xiao, H.-W., and Xiao, H.-Y.: Mist cannon trucks can exacerbate the formation of water-soluble organic aerosol and $PM_{2.5}$ pollution in the road environment, Atmos. Chem. Phys., 23, 6775-6788, 10.5194/acp-23-6775-2023, 2023b.

Xu, Y., Lin, X., Sun, Q. B., Xiao, H. W., Xiao, H., and Xiao, H. Y.: Elaborating the Atmospheric Transformation of Combined and Free Amino Acids From the Perspective of Observational Studies, J. Geophys. Res. Atmos., 129, 10.1029/2024jd040730, 2024a.

Xu, Y., Liu, T., Ma, Y.-J., Sun, Q.-B., Xiao, H.-W., Xiao, H., Xiao, H.-Y., and Liu, C.-Q.: Measurement report: Occurrence of aminiums in PM2.5 during winter in China – aminium outbreak during polluted episodes and potential constraints, Atmos. Chem. Phys., 24, 10531-10542, 10.5194/acp-

24-10531-2024, 2024b.

Xu, Y., Miyazaki, Y., Tachibana, E., Sato, K., Ramasamy, S., Mochizuki, T., Sadanaga, Y., Nakashima, Y., Sakamoto, Y., Matsuda, K., and Kajii, Y.: Aerosol Liquid Water Promotes the Formation of Water-Soluble Organic Nitrogen in Submicrometer Aerosols in a Suburban Forest, Environ. Sci. Technol., 54, 1406-1414, 10.1021/acs.est.9b05849, 2020.

Yang, T., Xu, Y., Ma, Y.-J., Wang, Y.-C., Yu, J. Z., Sun, Q.-B., Xiao, H.-W., Xiao, H.-Y., and Liu, C.-Q.: Field Evidence for Constraints of Nearly Dry and Weakly Acidic Aerosol Conditions on the Formation of Organosulfates, Environ. Sci. Technol. Lett., 10.1021/acs.estlett.4c00522, 2024.

Yang, T., Xu, Y., Ye, Q., Ma, Y.-J., Wang, Y.-C., Yu, J.-Z., Duan, Y.-S., Li, C.-X., Xiao, H.-W., Li, Z.-Y., Zhao, Y., and Xiao, H.-Y.: Spatial and diurnal variations of aerosol organosulfates in summertime Shanghai, China: potential influence of photochemical processes and anthropogenic sulfate pollution, Atmos. Chem. Phys., 23, 13433-13450, 10.5194/acp-23-13433-2023, 2023.

Yang, Y. R., Liu, X. G., Qu, Y., An, J. L., Jiang, R., Zhang, Y. H., Sun, Y. L., Wu, Z. J., Zhang, F., Xu, W. Q., and Ma, Q. X.: Characteristics and formation mechanism of continuous hazes in China: a case study during the autumn of 2014 in the North China Plain, Atmos. Chem. Phys., 15, 8165-8178, 10.5194/acp-15-8165-2015, 2015.

Yu, Q., Ding, X., He, Q., Yang, W., Zhu, M., Li, S., Zhang, R., Shen, R., Zhang, Y., Bi, X., Wang, Y., Peng, P. a., and Wang, X.: Nationwide increase of polycyclic aromatic hydrocarbons in ultrafine particles during winter over China revealed by size-segregated measurements, Atmos. Chem. Phys., 20, 14581-14595, 10.5194/acp-20-14581-2020, 2020.

Zhang, L., Li, J., Li , Y., Liu, X., ;, Luo, Z., Shen, G., and Tao, S.: Comparison of water-soluble and water-insoluble organic compositions attributing to different light absorption efficiency between

residential coal and biomass burning emissions Atmos. Chem. Phys., 24, 6323-6337, 10.5194/acp-24-6323-2024, 2024.

Zhang, L., Hu, B., Liu, X., Luo, Z., Xing, R., Li, Y., Xiong, R., Li, G., Cheng, H., Lu, Q., Shen, G., and Tao, S.: Variabilities in Primary N-Containing Aromatic Compound Emissions from Residential Solid Fuel Combustion and Implications for Source Tracers, Environ. Sci. Technol., 56, 13622-13633, 10.1021/acs.est.2c03000, 2022.

Zhang, Y., Zhang, R., Yu, J., Zhang, Z., Yang, W., Zhang, H., Lyu, S., Wang, Y., Dai, W., Wang, Y., and Wang, X.: Isoprene Mixing Ratios Measured at Twenty Sites in China During 2012–2014: Comparison With Model Simulation, J. Geophys. Res.Atmos., 125, 10.1029/2020jd033523, 2020.

Zhou, Y., Xing, X., Lang, J., Chen, D., Cheng, S., Wei, L., Wei, X., and Liu, C.: A comprehensive biomass burning emission inventory with high spatial and temporal resolution in China, Atmos. Chem. Phys., 17, 2839-2864, 10.5194/acp-17-2839-2017, 2017.

Zhu, Y., Yang, L., Chen, J., Wang, X., Xue, L., Sui, X., Wen, L., Xu, C., Yao, L., Zhang, J., Shao, M., Lu, S., and Wang, W.: Characteristics of ambient volatile organic compounds and the influence of biomass burning at a rural site in Northern China during summer 2013, Atmos. Environ., 124, 156-165, 10.1016/j.atmosenv.2015.08.097, 2016.